



Scale-Free Dynamics in Instantaneous Alpha Frequency Fluctuations: Validation, Test–Retest Reliability and Its Relationship with Task Manipulations

Huibin Jia^{1,2} · Xiangci Wu² · Enguo Wang² · Hua Wei³ · Fei Gao⁴

Received: 7 March 2022 / Accepted: 19 December 2022 / Published online: 7 January 2023
© The Author(s), under exclusive licence to Springer Science+Business Media, LLC, part of Springer Nature 2023

Abstract

Previous studies showed that scale-free structures and long-range temporal correlations are ubiquitous in physiological signals (e.g., electroencephalography). This is supposed to be associated with optimized information processing in human brain. The instantaneous alpha frequency (IAF) (i.e., the instantaneous frequency of alpha band of human EEG signals) may dictate the resolution at which information is sampled and/or processed by cortical neurons. To the best of our knowledge, no research has examined the scale-free dynamics and potential functional significance of IAF. Here, through three studies (Study 1: 25 participants; Study 2: 82 participants; Study 3: 26 participants), we investigated the possibility that time series of IAF exhibit scale-free property through maximum likelihood based detrended fluctuation analysis (ML-DFA). This technique could provide the scaling exponent (i.e., DFA exponent) on the basis of presence of scale-freeness being validated. Then the test–retest reliability (Study 1) and potential influencing factors (Study 2 and Study 3) of DFA exponent of IAF fluctuations were investigated. Firstly, the scale-free property was found to be inherent in IAF fluctuations with fairly high test–retest reliability over the parietal-occipital region. Moreover, the task manipulations could potentially modulate the DFA exponent of IAF fluctuations. Specifically, in Study 2, we found that the DFA exponent of IAF fluctuations in eye-closed resting-state condition was significantly larger than that in eye-open resting-state condition. In Study 3, we found that the DFA exponent of IAF fluctuations in eye-open resting-state condition was significantly larger than that in visual n-back tasks. The DFA exponent of IAF fluctuations in the 0-back task was significantly larger than in the 2-back and 3-back tasks. The results in studies 2 and 3 indicated that: (1) a smaller DFA exponent of IAF fluctuations should signify more efficient online visual information processing; (2) the scaling property of IAF fluctuations could reflect the physiological arousal level of participants.

Keywords Instantaneous alpha frequency · Scale-free · Long-range temporal correlations · Resting-state · Working memory load · Detrended fluctuation analysis

Handling Editor: Dr. Micah M. Murray.

Huibin Jia and Xiangci Wu have contributed equally to this work and share first authorship.

✉ Enguo Wang
enguowang@126.com

✉ Hua Wei
weihuaweihua@163.com

✉ Fei Gao
gaofei19780318@sina.com

² School of Psychology, Henan University, Kaifeng 475004, China

³ Department of Psychology, Suzhou University of Science and Technology, Suzhou 215009, China

⁴ Department of Pain Medicine, Peking University People's Hospital, Beijing 100044, China

¹ Institute of Cognition, Brain and Health, Henan University, Kaifeng 475004, China

Introduction

The alpha band is the dominant frequency band, especially during the task-free eye-closed (EC) state and over the parietal-occipital region, in the human scalp electroencephalography (EEG) of adults (Dickinson et al. 2018). It is manifested by a peak around 10 Hz in spectral analysis (e.g., Fourier transform) and is an oscillatory component (i.e., the so-called “alpha wave” or “Berger’s wave”) of the EEG signal which is well recognized since 1930s (Adrian and Matthews 1934). Exploring the features of alpha oscillations (e.g., individual alpha peak frequency, magnitude, and frequency range) has generated considerable interest, in particular with regards to the modulation effects of demographic, cognitive, emotional, physiological, genetic, psychomotor and psychiatric variables (Ahern and Schwartz 1985; Dickinson et al. 2018; Gabard-Durnam et al. 2013; Hu et al. 2013; Klimesch 1999; Nieber and Schlegel 1992; Zietsch et al. 2007). The magnitude and peak frequency of alpha oscillations, along with those of other EEG oscillations, vary over time during a single EEG recording: they are non-stationary (Berthouze et al. 2010; Haegens et al. 2014). In order to probe the dynamic characteristics of alpha waves, a number of time-frequency analysis techniques (e.g., short-time Fourier transform, discrete/continuous wavelet transforms, and band-pass filtering + Hilbert transform) have been developed and utilized in empirical research (Berthouze et al. 2010; Jia et al. 2015). Extensive preceding research in this field has been dedicated to understanding the dynamics of instantaneous alpha magnitude (IAM) and its relation to different factors, such as demographic variables and task manipulations (Berthouze et al. 2010; Montez et al. 2009; Peng et al. 2012). As far as we know, only a few studies have investigated the functional role and determinants of instantaneous alpha frequency (IAF) (Nelli et al. 2017; Samaha and Postle 2015). There is an increasing amount of experimental evidence that suggests that IAF fluctuations are significant even on very short time scales (e.g. 1 s). IAF fluctuations appear to influence regional cerebral blood flow in a brain network consisting of regions associated with the control of attention and readiness for external stimuli (Jann et al. 2010). Theories suggest that the fluctuations of IAF is a coding scheme in which self-regulation of IAF during a single EEG recording time may dictate the resolution at which information is sampled and/or processed by cortical neurons (Cecere et al. 2015; Samaha et al. 2015; Samaha and Postle 2015).

Converging research suggests that the human brain operates at the cusp of dynamic instability, as signified by scale-free temporal auto-correlations (ACs) (also named as power-law-form long-range temporal correlations

[LRTC]) (Linkenkaer-Hansen et al. 2001). Supposing $AC(\tau)$ is the AC at time τ and s is the scaling factor, the $AC(\tau)$ and $AC(s \times \tau)$ obey the following power law: $AC(s \times \tau) = s^{2H} \times AC(\tau)$, which suggests that if time τ is rescaled to $s \times \tau$, then the shape of ACs preserves and only rescales by a factor s^{2H} (He 2011). The scaling exponent H provides a quantitative measure of temporal dependencies in neural oscillations of different time scales and could be assessed by the rescaled range (R/S) analysis and the more robust detrended fluctuation analysis (DFA) (Lei et al. 2013; Smit et al. 2011). This scale-free/scale-invariant behavior has been detected in biomedical signals from a wide range of physiological phenomena, which suggests that the structure of a given biomedical signal repeats itself on subintervals of this signal: they are self-similar (Ciuciu et al. 2014; Hardstone et al. 2012; Jia et al. 2018; Jia and Yu 2019). Further, it was shown that the scaling property of biomedical signals can be modulated by various factors, such as age, genetic inheritance, neurological disorders, personality traits and task manipulations (Berthouze et al. 2010; Hahn et al. 2012; He 2011; Jia et al. 2018; Lei et al. 2013; Linkenkaer-Hansen et al. 2007; Smit et al. 2011). The presence of scale-free dynamics supports the hypothesis that the brain operates in a critical state, i.e., its dynamics may be positioned at the border between spatiotemporal order and disorder, reminiscent of non-equilibrium phase transitions in thermodynamic systems. This has been suggested to be associated with optimized information processing and computation (Shew and Plenz 2013). As for the EEG alpha oscillations, numerous studies have confirmed the presence of scale-free phenomenon in instantaneous alpha magnitude (IAM) fluctuations (Berthouze et al. 2010; Montez et al. 2009; Smit et al. 2011). However, there is no knowledge on whether the temporal fluctuations of IAF also exhibit scale-free behavior. Here, the presence of scale-freeness in the fluctuations of IAF was confirmed using three studies. This indicates that the temporal fluctuations of IAF are associated with optimized information processing and computation during cognitive activities.

Moreover, we evaluated the test–retest reliability of the scaling exponent (i.e., DFA exponent here) of IAF fluctuations, since the test–retest reliability is a critical property of any features of neural signals. An EEG feature with high test–retest reliability is reliable, and then attempts to quantify its changes through experimental manipulations are trustworthy as its changes could reflect task-related neuronal dynamics. An EEG feature with relatively higher test–retest reliability could be used as a stable neurophysiological “trait” biomarker reflecting anatomical properties of the human brain.

Here, using the maximum likelihood based detrended fluctuation analysis (ML-DFA), which could provide the

scaling exponent (i.e., DFA exponent here) on the basis of presence of scale-free behavior being validated (Botcharova et al. 2013), the following three questions were investigated: (1) Alike the IAM fluctuations, whether scale-free characteristic could be detected in the IAF fluctuations? (2) Does the scale-free feature of IAF fluctuations, quantified by DFA exponent, exhibit substantial high test–retest reliability? (3) Could the scale-free behavior of IAF fluctuations be modulated by task manipulations (e.g., eye status [eye-open (EO) or EC], visual working memory loads)? Moreover, are these effects immune from the value of other features of alpha oscillations, such as alpha magnitude, peak alpha frequency (PAF) and DFA exponent of IAM?

Materials and Methods

Study 1 The Presence of Scale-Free Behavior in IAF Fluctuations and Its Test–Retest Reliability

Participants

The EEG data were collected from 25 healthy right-handed volunteers (13 females), aged 21 ± 1.9 years (mean \pm SD, range 16–25 years). All participants gave their written informed consent and were paid for their participation. The experimental procedure was conducted according to the Helsinki declaration and was approved by the local ethics committee of Peking University People's Hospital. The dataset and/or MATLAB code of Study 1 are available from the corresponding authors upon reasonable request subject to a formal data sharing agreement with Prof. Fei Gao.

EEG Recording

To collect resting EEG data, each participant was required to sit in a comfortable chair in a silent, temperature-controlled room, and was instructed to keep relaxed and their eyes closed. Two sessions of EEG datasets, each lasting about 5 min, were recorded. The first session (session 1) and the second session (session 2) were recorded at 9:00 am and 10:00 am on the same day, respectively.

The EEG data of 20 Ag/AgCl scalp electrodes (i.e., Fp1, Fp2, F7, F3, Fz, F4, F8, T3, C3, Cz, C4, T4, T5, P3, Pz, P4, T6, O1, Oz and O2) arranged according to the international 10–20 system (ASA-Lab, ANT B.V., Netherlands) were recorded. The online recording parameters can be summarized as follows: (1) the impedances of all electrodes were kept below than 10 K Ω ; (2) the average of left and right mastoids was used as online reference; (3) the EEG signals were amplified and band-pass filtered with 0.1–100 Hz, and finally transferred into digital signals with sampling rate 256 Hz.

EEG Data Preprocessing

The EEG data were preprocessed using the EEGLAB software (<https://sccn.ucsd.edu/eeglab/index.php>) (Delorme and Makeig 2004), which is an easily extensible, highly evolved, and widely used open source environment for signal processing and visualization of electroencephalographic data running on MATLAB (The Mathworks, Inc.). The preprocessing involves the following steps. Firstly, the raw continuous EEG data was band-pass filtered between 0.5 and 80 Hz through a Hamming windowed finite impulse response (FIR) filter, whose order was determined as the number of sampling points of three cycles of the lower edge of the band considered (i.e., 0.5 Hz). A notch filter was used to eliminate 50 Hz line noise. These operations were done through the EEGLAB function “*pop_eegfiltnew*”. Secondly, electrodes with relatively low signal-to-noise ratio (i.e., “bad electrodes”) were identified through visual inspection of the filtered EEG data and interpolated using a spherical spline method in the EEGLAB function “*pop_interp*”. The mean and standard deviation of electrodes interpolated across subjects were 3.5 and 1.2, respectively. Thirdly, the data portions contaminated by electrooculogram (EOG) and electromyography (EMG) were corrected using the Blind Source Separation (BSS) algorithm through the function “*pop_autobsseog*” and “*pop_autobssemg*” respectively in the automatic artifact removal (AAR) toolbox (https://github.com/germangh/eeglab_plugin_aar). Fourthly, EEG data were remontaged against the common average reference, and segmented into epochs with a length of 2000 ms. Lastly, EEG epochs still contaminated by any physiological or non-physiological artifacts or with amplitude values exceeding ± 80 μ V at any electrode were rejected.

Extracting the IAF

In practical IAF extraction, the IAF is commonly defined as the first derivative in time of the phase of the alpha-band EEG signal, or the change in phase per unit time as time approaches zero. Similarly to the approaches used in previous studies, for example Nelli et al. (2017) and Cohen (2014), the IAF fluctuations of each electrode, each session and each participant were estimated via the following steps (Cohen 2014; Nelli et al. 2017).

Firstly, the preprocessed EEG signals were band-pass filtered between 8 and 13 Hz using a FIR filter with an order 96 (i.e., the sampling point number of three cycles of 8 Hz). The lower and upper limits of this band-pass filter were determined by the results of power spectra analysis conducted over each electrode, each session, and each participant using fast Fourier transformation (FFT). We found that alpha peak in power spectra could be clearly seen in the occipital regions for all participants. Observing the power

spectra, we found that the peak alpha frequency (PAF) was located between 9 and 11 Hz. Thus, the alpha band limit was set to be 8–13 Hz.

Secondly, the phase time series was estimated through the Hilbert transform, which was then unwrapped to be cumulative so that there were no discontinuities at $-\pi$ and π . The IAF was calculated as the first derivative of the unwrapped phase angles. To convert to units of hertz (Hz), the IAF fluctuations calculated above were multiplied by the data sampling rate in hertz and then divided by $2 * \pi$. To sum up, in MATLAB code the IAF of 8–13 Hz band-pass filtered signal “data” with sampling rate “fs” can be calculated as $fs * \text{diff}(\text{unwrap}(\text{angle}(\text{hilbert}(\text{data})))) / (2 * \pi)$.

Lastly, the median filter was applied to attenuate non-physiological noise spikes in IAF fluctuations. A small noise in the phase angle time series may lead to a large spike in the IAF fluctuations (e.g., from 10 to 100 Hz, even to -100 Hz in just a few milliseconds). In order to deal with these occasional sharp discontinuities and attenuate the influence of fluctuations far outside of the band-pass range, a median filter which outperformed mean-based or convolution-based smoothing filters when the noise spikes are extreme was adopted. In the median filter, the sliding window method was applied to compute the moving median. As suggested by Cohen (2014), the median filter was utilized several times with different window widths (i.e., from 10 to 400 ms with an order of 10), and then the mean value of these median filters was taken (Cohen 2014).

The ML-DFA

Here, the ML-DFA technique was used to validate the presence of scale-invariance in IAF fluctuations, and compute the DFA exponent introduced by Peng et al. (1995). The procedure for the IAF fluctuations of each electrode, each session and each participant can be summarized as follows (Botcharova et al. 2013; Peng et al. 1995).

Firstly, compute the signal profile of each IAF fluctuations. The signal profile of the IAF fluctuations at time point t can be computed via the following formula: $X(t) = \sum_{k=1}^t Y(k) - \langle Y \rangle$, where $\langle Y \rangle$ is the mean value of IAF fluctuations $Y(t)$. It has been shown that this operation can eliminate the global trend of the signal and ensure the stationarity of the time series being investigated.

Secondly, define a set of window sizes T , which are equally spaced on a logarithmic scale between 2 and 15 s, and then compute “fluctuation function” for each window size. For each window size $t \in T$, the whole signal profile was split into windows with a length of t and 50% overlap. Then, the standard deviation of each window with length t was calculated after its linear trend was removed through a least-squares fit. The mean standard deviation of all windows

with length t was defined as the fluctuation function $F \langle t \rangle$ of window size t .

Thirdly, plot the fluctuation function for all window sizes on double logarithmic axes, which was named as the *DFA fluctuation plot*. The presence of scale-invariance or power law will result in linear scaling in this DFA fluctuation plot. Here, a maximum likelihood-based model selection technique (i.e., ML-DFA) was used to assess the validity of linearity in DFA fluctuation plot. In this technique, a set of alternative models, including linear, quadratic, cubic, quartic, quantic, square root, cube root, fourth root, exponential, logarithmic and spline with 2–4 linear sections, were fitted to the DFA fluctuation plot. The most appropriate model was believed to be the one with the lowest value of the Akaike Information Criterion (AIC) and Bayesian Information Criterion (BIC), i.e., the model that provided the best explanation of the data without over-fitting it (Botcharova et al. 2013; Jia and Yu 2019). The presence of scale-free behavior was validated only if the linear model was selected as the most appropriate model by both AIC and BIC.

Lastly, the slope of the least-squares line in the DFA fluctuation plot was termed as the DFA exponent, which was commonly interpreted as an estimation of the Hurst exponent. DFA exponents in the 0–0.5 range and 0.5–1.0 range indicate anti-correlation (i.e., fluctuation functions are smaller in larger time windows than expected by chance) and positive correlation respectively. Uncorrelated signals (e.g., white noise) have a DFA exponent of 0.5. The DFA exponent of non-stationary signals is larger than 1.0 (Hardstone et al. 2012; Jia and Yu 2019).

Evaluating the Test–Retest Reliability of Scaling Exponent of IAF

In order to estimate the test–retest reliability (i.e., reproducibility) of DFA exponents across sessions, the intra-class correlation (ICC) which integrated both intra-individual variability and inter-individual variability was calculated for each electrode (Chen et al. 2015). ICC was defined as $\sigma_w^2 / (\sigma_b^2 + \sigma_w^2)$, where σ_w^2 and σ_b^2 was intra-individual variability and inter-individual variability respectively. As can be seen from this formula, lower intra-individual variability or higher inter-individual variability will lead to higher test–retest reliability and vice versa. The variance components were estimated in linear mixed models (LMMs) with the restricted maximum likelihood (ReML) approach. An ICC value approaching 1 indicates high reproducibility, while a value close to 0 indicates very low reproducibility. According to the classifying criteria of intra-class correlation (ICC) value shown in Sampat et al. (2006), values less than 0.4 indicated low reliability, values 0.4 to 0.6 indicated fair reliability, values

0.6 to 0.75 indicated good reliability, and values 0.75 to 1.0 indicated excellent reliability (Sampat et al. 2006).

Testing the Relationship Between DFA Exponent of IAF and that of Instantaneous Alpha Magnitude (IAM)

Here, we statistically tested the relationship between DFA exponent of IAF and that of instantaneous alpha magnitude (IAM). Firstly, the DFA exponent of IAM of each electrode, each session, and each participant was estimated using exactly the same DFA settings in IAF analysis. Here, IAM fluctuations were evaluated via the Hilbert transform. Assuming $X(t)$ and $X_H(t)$ are the band-pass (8–13 Hz) filtered signals and its Hilbert transform at sampling time t respectively, we could obtain the analytic signal $X_{an}(t)$ via the following equation: $X_{an}(t) = X(t) + i \cdot X_H(t)$. The IAM of $X(t)$ is computed as the modulus of $X_{an}(t)$. Secondly, the Pearson correlation coefficient between the DFA exponent of IAF fluctuations and that of IAM fluctuations was computed for each electrode and each session respectively.

Study 2 The DFA Exponent of IAF Fluctuations in EO and EC Resting State

Participants

Here, 82 undergraduate students (34 male with mean age 20.89 ± 2.04 years; 48 female with mean age 21 ± 1.80 years) from Nanjing University, Nanjing, China were selected as participants. All participants had normal or corrected visual acuity, no psychiatric disorders, and gave their written informed consent. This study was carried out in accordance with the basic principles of the Declaration of Helsinki and approved by the local research ethics committee of Nanjing University. The datasets and/or MATLAB code of Study 2 are available from the corresponding authors upon reasonable request subject to a formal data sharing agreement with Dr. Hua Wei.

EEG Recording

The EO and EC EEG data (each lasting about 3 min) were recorded via a 32-channel SynAmps recording system (Neuroscan Labs, Sterling, VA) and a standard EEG cap based on the extended 10–20 system, with a pass-band of 0.01–100 Hz and a sampling rate of 500 Hz. During online recording, the electrode AFz was used as the online reference, and the impedances of all the electrodes were below 10 K Ω .

EEG Data Analysis

Firstly, same as Study 1, the EEG data were preprocessed using EEGLAB with exactly the same pipeline and MATLAB functions. Note that, the mean and standard deviation of bad electrodes across subjects were 2.3 and 0.6, respectively. Then, according to the steps illustrated in Study 1, the IAF fluctuations were extracted. Since the results of Study 1 showed that the intra-class correlation (ICC) values of the DFA exponent of the occipital electrodes were much higher than the electrodes over the other scalp regions (see “Results of Study 1” section), only the IAF fluctuations of the occipital electrode Oz was analyzed here. Lastly, the presence of scale-invariance in IAF fluctuations was validated by the ML-DFA technique, and DFA exponents of these time series were computed.

In the current study, the following hypothesis was tested: whether a significant conditional difference could be detected between the DFA exponents of the IAF of the EO condition and the EC condition? Moreover, could this statistical effect be modulated by other alpha features, including the peak alpha frequency (PAF), magnitude of alpha band, and DFA exponent of instantaneous alpha magnitude (IAM)? Note that the PAF and alpha magnitude were calculated as the time-averaged value of IAF and IAM fluctuations respectively.

Study 3 The Effect of Visual Working Memory Load on the DFA Exponent of IAF Fluctuations

Participants

The current study included EEG and behavioral data from 26 right-handed healthy participants (9 males, mean age 26.1 ± 3.5 years). Participants were informed about the procedure of the experiment and gave written informed consent prior to the experiment. This study was conducted according to the Helsinki declaration and was approved by the Ethics Committee of the Institute of Psychology and Ergonomics at the Berlin Institute of Technology (Shin et al. 2018). The datasets of Study 3 are available at http://doc.ml.tu-berlin.de/simultaneous_EEG_NIRS/.

Experimental Procedure

The participants were required to sit on a comfortable chair at about 120 cm from a 24" LCD monitor in a silent, temperature-controlled room. They were instructed to keep their eyes fixed on the stimulus presented in the middle of the screen throughout the experiment, and to put their index and middle fingers on numbers 7 and 8 of the numeric keypad buttons respectively.

The participants were required to complete a visual n-back task with three levels: 0-back, 2-back, and 3-back. Each level task was repeated three times. Thus, nine series of n-back tasks with a counterbalanced order (i.e., $0 \rightarrow 2 \rightarrow 3 \rightarrow 2 \rightarrow 3 \rightarrow 0 \rightarrow 3 \rightarrow 0 \rightarrow 2$) were performed for each participant. In each series, firstly an instruction showing the level of the task (i.e., 0-, 2-, or 3-back) was presented on the center of screen. Then, the participants should complete 20 trials (30% targets, 70% non-targets), lasting 40 s (referred to as the 0-, 2-, or 3-back task segment in the following data analysis). In each trial, a one-digit number was displayed for 0.5 s, followed by a fixation cross lasting 1.5 s. In the 2- or 3-back condition, if the number displayed currently matched the 2 or 3 preceding numbers respectively, they should press number 7; otherwise, they should press number 8. In the 0-back condition, the participants were asked to press number 7 or number 8 when they saw the number. At the end of each series, the participants were asked to relax and gaze at the fixation cross in the middle of the screen for 20 s (referred to as the rest segment in the following data analysis) (Shin et al. 2018).

EEG Recording

EEG data was recorded using a BrainAmp EEG amplifier (Brain Products GmbH, Gilching, Germany) with sampling rate 1000 Hz. Thirty EEG active electrodes were montaged according to the international 10–5 system with a standard EEG cap. For more information, see Shin et al. (2018) (Shin et al. 2018).

EEG Data Analysis

The EEG data were preprocessed using EEGLAB with the following steps. Firstly, the raw continuous EEG data was band-pass filtered between 1 and 30 Hz through a Hamming windowed FIR filter and downsampled to 250 Hz. Secondly, “bad electrodes” were identified through visual inspection and interpolated using a spherical spline method in EEGLAB. The mean and standard deviation of electrodes interpolated across participants were 4.2 and 1.3, respectively. Thirdly, the data portions contaminated by physiological and non-physiological artifacts were corrected using independent component analysis (ICA). Fourthly, EEG data were remontaged against common average reference. Lastly, the 0-back task segments, the 2-back task segments, the 3-back task segments, and the rest segments were extracted. Note that, for each participant, the total length of the 0-, 2- or 3-back task segments was 120 s ($40 \text{ s/segment} \times 3 \text{ segments} = 120 \text{ s}$), whereas the total length of the rest segments was 180 s ($20 \text{ s/segment} \times 9 \text{ segments} = 180 \text{ s}$).

After the EEG data were preprocessed, the IAF fluctuations of the occipital electrodes O1 and O2 were extracted

for four kinds of segments (i.e., rest, 0-back, 2-back, and 3-back) respectively using the procedures illustrated in Study 1 and Study 2. The presence of scale-invariance in IAF fluctuations was validated by the ML-DFA technique, and then DFA exponents of these time series were computed. The DFA exponents of electrodes O1 and O2 were calculated respectively, and then averaged across these two electrodes.

Here, in order to test the effect of distinct working memory loads (i.e., rest, 0-back, 2-back and 3-back) on the DFA exponent of IAF fluctuations, one-way repeated measure ANOVA with working memory load as within-subject factor was conducted. Moreover, one-way analysis of covariance (ANCOVA) with working memory loads as within-subject factor, the PAF, magnitude of alpha band, and DFA exponent of instantaneous alpha magnitude (IAM) as covariates was also performed. In both the ANOVA and ANCOVA, if the main effect was significant (i.e., $p < 0.05$), post hoc comparisons were made to determine the significance of pairwise contrasts by using the Bonferroni procedure ($\alpha = 0.05$).

In order to test the relationship between the DFA exponent of IAF fluctuations and behavioral data in the n-back task, the Pearson’s correlation coefficients between the DFA exponent of IAF fluctuations and reaction time (RT) in the 0-back condition, 2-back condition, and 3-back condition were computed. The significance of the correlation coefficients was assessed with t-statistic. The threshold for significance was $p < 0.05$.

Results

Results of Study 1

In Study 1, we tested whether scale-free dynamics could be detected in the IAF fluctuations. Moreover, if this hypothesis is validated, does the scaling exponent of IAF fluctuations exhibit relatively high test–retest reliability? In order to validate the presence of scale-invariance in IAF fluctuations, the ML-DFA technique was applied. Then, the intra-class correlation (ICC) was used to evaluate the test–retest reliability of scaling exponent (i.e., the DFA exponent) across sessions.

The ML-DFA conducted in Study 1 found that the presence of scale-invariance was validated for the IAF fluctuations of all the participants, except the IAF fluctuations of electrode Oz of participant # 17 in session 1 and electrode F7 of participant # 11 in session 2. This result was also confirmed by a high value of the coefficient of determination (i.e., $R^2 > 0.95$ for all the IAF fluctuations) of the least-squares line in the DFA fluctuation plot (Figs. 1 and 2).

The scalp distribution of the grand average DFA exponent of IAF fluctuations of session 1 and session 2 are shown in panels a and b of Fig. 3, respectively. The ICC values of the

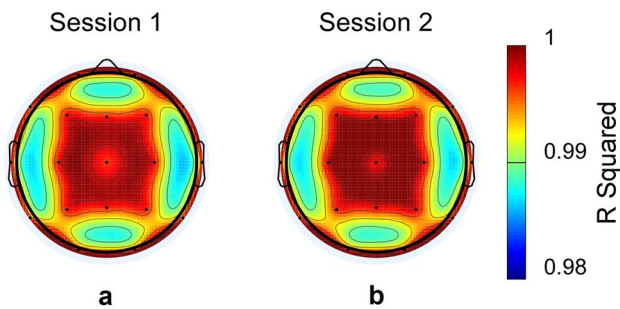


Fig. 1 The scalp distribution of grand average R squared (i.e., R^2) value of the least-squares line of the DFA fluctuation plot when evaluating the scaling exponent of instantaneous alpha frequency (IAF) fluctuations in Study 1 (**a** session 1; **b** session 2)

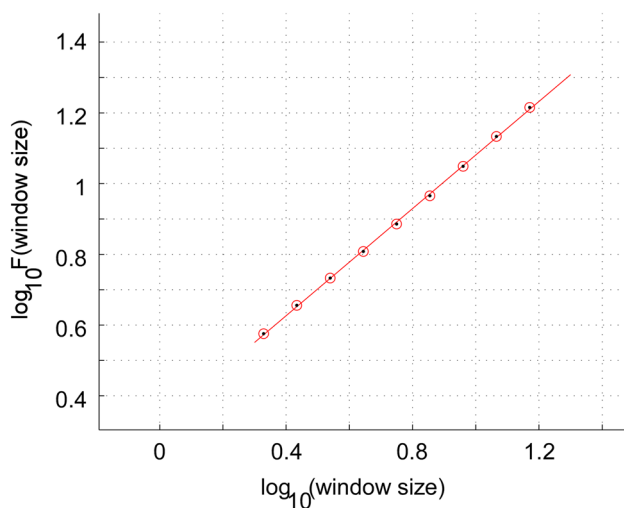


Fig. 2 The DFA fluctuation plot of instantaneous alpha frequency (IAF) fluctuations of electrode Oz of a typical participant in session 1 of Study 1

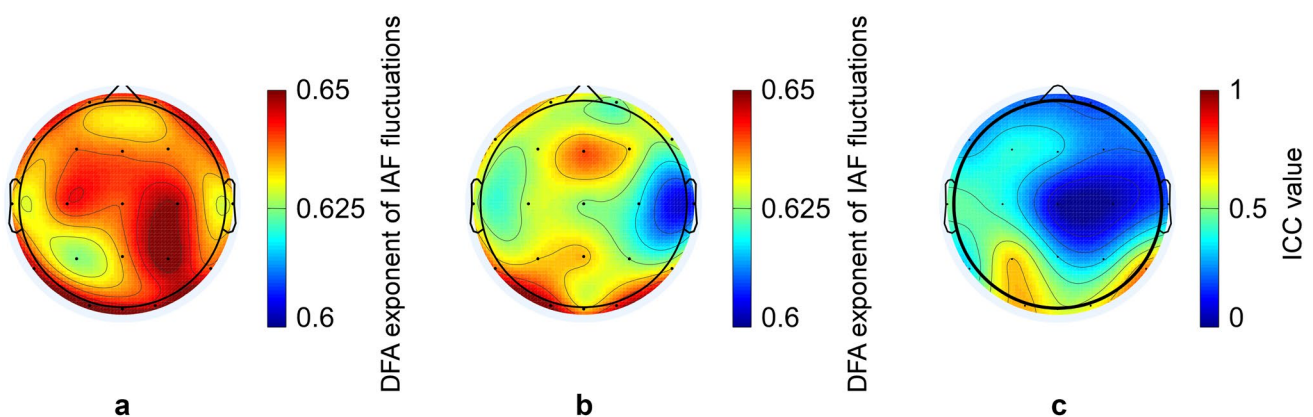


Fig. 3 The scalp distribution of the grand average DFA exponent of instantaneous alpha frequency (IAF) fluctuations of session 1 and session 2 (**a** and **b** respectively), and the intra-class correlation (ICC) value of the DFA exponent of IAF fluctuations (**c**) in Study 1

DFA exponent of IAF fluctuations for each electrode are displayed in Fig. 3. This shows that the ICC values are highest over parietal-occipital electrodes. The DFA exponents of IAF fluctuations of parietal-occipital electrodes have “good reliability” according to the classifying criteria in Sampat et al. (2006) (P3: 0.67; Oz: 0.58; O1:0.70; O2: 0.60; P8: 0.75). These results showed that the scale-free feature of IAF fluctuations exhibits substantial high test–retest reliability.

We also tested the relationship between the scaling exponents of IAF and those of instantaneous alpha magnitude (IAM) using the Pearson correlation coefficient. We found that significantly positive correlations could be found on nearly all of the electrodes for both sessions except for electrode Cz. For session 1, the mean value and standard deviation of the Pearson correlation coefficients across electrodes were 0.47 and 0.12, respectively. For session 2, the mean value and standard deviation of the Pearson correlation coefficients across electrodes were 0.56 and 0.10, respectively.

Results of Study 2

In Study 2, we tested whether scale-free dynamics could be detected in the IAF fluctuations via EEG datasets from another cohort using the ML-DFA technique. Further, we investigated whether the scale-free behavior of IAF fluctuations could be modulated by eye status (open vs. closed). We also investigated the relationship between the DFA exponent of IAF fluctuations and other features of alpha oscillations (i.e., alpha magnitude, PAF, and the DFA exponent of instantaneous alpha magnitude [IAM]) using Pearson correlation coefficients.

The ML-DFA conducted in Study 2 revealed that the presence of scale-invariance was validated for the IAF fluctuations of all the participants in both the EC and EO condition.

The DFA exponents of IAF fluctuations across all the electrodes, conditions, and participants were larger than 0.5 and smaller than 1.0, which suggests that the IAF fluctuations are positively correlated (i.e., fluctuation functions are larger in larger time windows than expected by chance).

After the DFA exponents of IAF fluctuations for the occipital electrode were computed, a paired t-test with eye status (2 levels: EC and EO) as the independent variable was conducted. A significant conditional difference was detected between the DFA exponents of IAF fluctuations of the EC condition and the EO condition (EC: 0.66 ± 0.075 , EO: 0.62 ± 0.05 ; $t(81) = 4.9$, $p < 0.001$). The DFA exponent of IAF fluctuations of occipital electrodes in the EC condition was significantly larger than that in the EO condition

(panel a of Fig. 4). We investigated whether this statistical effect could be modulated by the PAF, magnitude of alpha oscillations, and DFA exponent of IAM. For the PAF (panel b of Fig. 4), we found that: (1) The PAF of EC and EO condition was not significantly different, as revealed by a paired t-test with eye status (2 levels: EC and EO) as independent variable (EC: 10.32 ± 0.43 Hz, EO: 10.37 ± 0.28 Hz; $t(81) = -1.28$, $p > 0.05$); (2) the Pearson correlation coefficients between PAF and DFA exponent of IAF fluctuations were not significant both for the EC condition ($r = -0.02$, $p > 0.05$) and the EO condition ($r = 0.03$, $p > 0.05$). For the magnitude of alpha oscillations (panel c of Fig. 4), we found that: (1) the alpha magnitude of the EC and EO condition was significantly different, as revealed by a paired

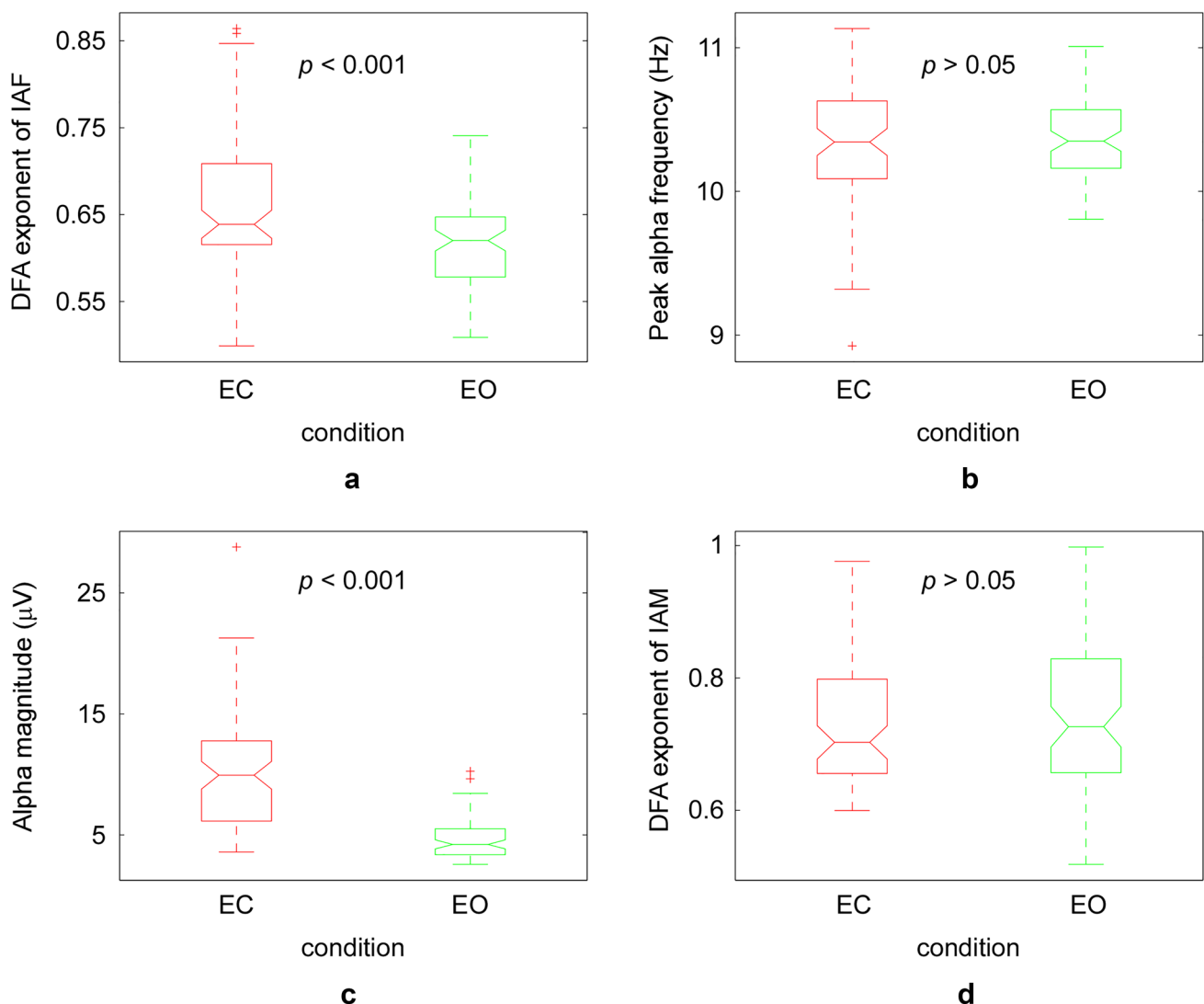


Fig. 4 The DFA exponent of instantaneous alpha frequency (IAF) fluctuations (a), the peak alpha frequency (b), the alpha magnitude (c), and the DFA exponent of instantaneous alpha magnitude (IAM) fluctuations (d) in eye-closed (EC) and eye-open (EO) resting-state

condition. Compared to the EO condition, the DFA exponent of IAF fluctuations and alpha magnitude were significantly larger in the EC condition

t-test with eye status (2 levels: EC and EO) as the independent variable (EC: $10.17 \pm 4.78 \mu\text{V}$, EO: $4.64 \pm 1.62 \mu\text{V}$; $t(81) = 12.45$, $p < 0.001$); (2) the Pearson correlation coefficients between alpha magnitude and DFA exponent of IAF fluctuations were not significant both for EC condition ($r = 0.16$, $p > 0.05$) and EO condition ($r = 0.14$, $p > 0.05$). For the DFA exponent of IAM (panel d of Fig. 4), we found that: (1) the DFA exponent of IAM of EC and EO condition was not significantly different, as revealed by a paired t-test with eye status (2 levels: EC and EO) as the independent variable (EC: 0.75 ± 0.12 , EO: 0.74 ± 0.12 ; $t(81) = 0.27$, $p > 0.05$); (2) the Pearson correlation coefficients between DFA exponent of IAF and that of IAM were significant both for EC condition ($r = 0.27$, $p < 0.05$) and EO condition ($r = 0.25$, $p < 0.05$).

Moreover, we found that a significant conditional difference (i.e., the DFA exponent of the EC condition was significantly larger than that of the EO condition) could also be observed when the PAF, alpha magnitude, and DFA exponent of IAM were included as covariates. These results showed that the scale-free behavior of IAF fluctuations could be modulated by the eye status (EO vs. EC) of participants, which is immune from the value of other features of alpha oscillations.

Results of Study 3

In Study 3, we tested whether scale-free dynamics could be detected in the IAF fluctuations via EEG datasets from the third cohort using the ML-DFA technique. Further, we investigated whether the scale-free behavior of IAF fluctuations could be modulated by visual working memory loads (rest, 0-back, 2-back, and 3-back) of participants using ANOVA and ANCOVA. We also investigated the potential links between the DFA exponent of IAF fluctuations and behavioral performance (i.e., the reaction time [RT]).

The ML-DFA conducted in Study 3 revealed that: the presence of scale-invariance was validated for all the IAF fluctuations of all participants, except for electrode O1 of one participant under 0-back and 2-back condition.

Both the ANOVA and ANCOVA conducted on the DFA exponents of IAF fluctuations found that the main effect of working memory load was significant (Fig. 5): $F(3,72) = 15.05$, $p < 0.01$ (ANOVA) and $F(3,72) = 8.47$, $p < 0.01$ (ANCOVA). Post hoc tests of ANOVA/ANCOVA revealed that: (1) the DFA exponent of IAF fluctuations in the rest condition was significantly larger than that in the 0-back condition, 2-back condition and 3-back condition; (2) the DFA exponent of IAF fluctuations in the 0-back condition was significantly larger than that in the 2-back condition and 3-back condition; (3) the DFA exponent of IAF fluctuations in the 2-back condition and 3-back condition

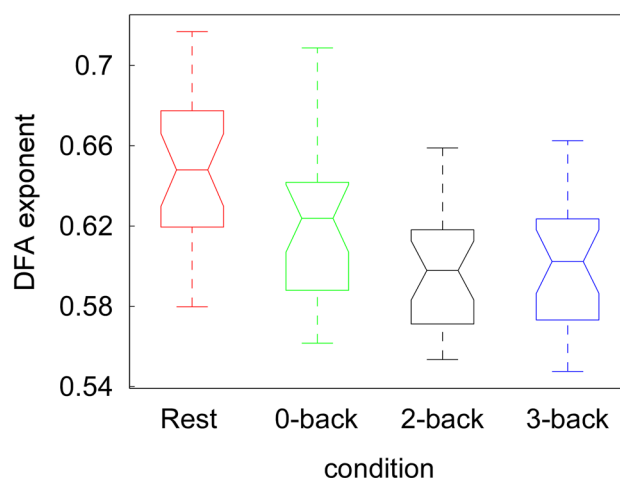


Fig. 5 The DFA exponent of instantaneous alpha frequency (IAF) fluctuations of the eye-open (EO) resting-state condition, 0-back condition, 2-back condition and 3-back condition in the visual n-back task. The DFA exponent of IAF fluctuations in the EO condition was significantly larger than those in the 0-back condition, 2-back condition, and 3-back condition. The DFA exponent of IAF fluctuations in the 0-back condition was significantly larger than those in the 2-back condition and the 3-back condition

was not significantly different. As shown in Fig. 6, the Pearson's correlation coefficient between DFA exponent of IAF fluctuations and RT in 0-back condition was significant ($r = 0.52$, $p < 0.01$, as shown in panel a of Fig. 6), whereas that in 2-back condition and 3-back condition were not significant ($r = 0.08$, $p > 0.05$ and $r = 0.09$, $p > 0.05$ respectively, as shown in panel b and panel c of Fig. 6). Moreover, we found that removing the outliers did not significantly alter the results (0-back: $r = 0.37$, $p < 0.05$; 2-back: $r = 0.09$, $p > 0.05$; 3-back: $r = 0.07$, $p > 0.05$). These results showed that the scale-free behavior of IAF fluctuations could be modulated by visual working memory loads of participants.

Discussion

In the current study, the scale-free characteristic of IAF fluctuations was investigated. Firstly, through ML-DFA procedures conducted on the resting-state EEG datasets of Study 1 and Study 2 and the event-related EEG datasets of Study 3, we found that scale-free behavior was inherent in IAF fluctuations. Secondly, the test–retest reliability of DFA exponent of IAF fluctuations was fairly high over parietal-occipital regions. Thirdly, the eye-status (i.e., EC vs. EO resting-state condition) and the working memory loads in n-back task could modulate the DFA exponent of IAF fluctuations. In Study 2, compared with the EC resting-state condition, the DFA exponent of IAF fluctuations

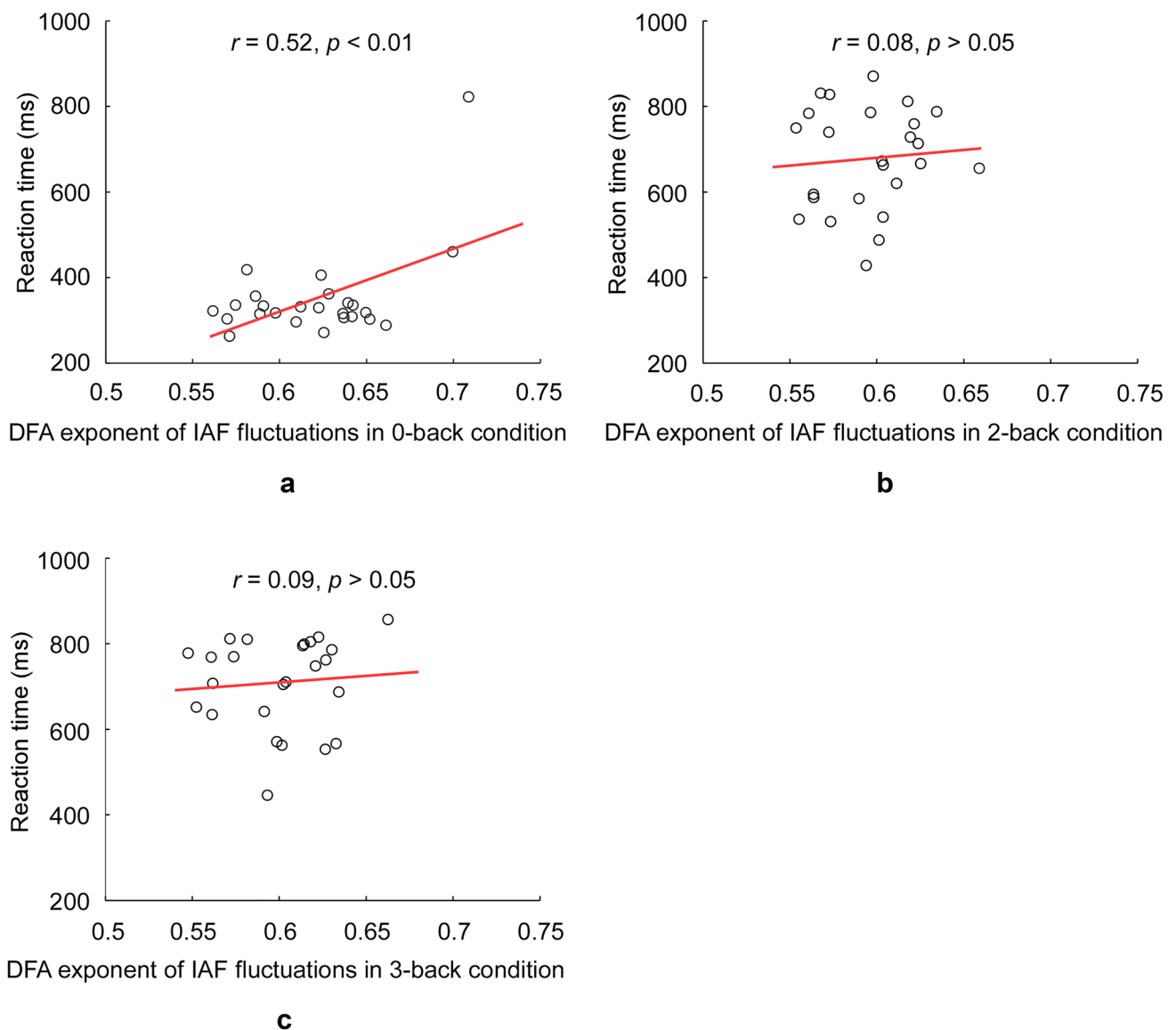


Fig. 6 The relationship between the DFA exponent of instantaneous alpha frequency (IAF) fluctuations and reaction time (RT) in the 0-back condition (a), 2-back condition (b) and 3-back condition (c) of the visual n-back task. The Pearson's correlation coefficient between

the DFA exponent and RT in 0-back condition was significant, whereas those in the 2-back condition and the 3-back condition were not significant (i.e., $p > 0.05$)

was found to be significantly lower in the EO resting-state condition. Moreover, this effect is immune from the values of other features of alpha oscillations, including the peak alpha frequency (PAF), alpha magnitude, and DFA exponent of instantaneous alpha magnitude (IAM). In Study 3, we found that, compared with the EO resting-state condition, the DFA exponent of IAF fluctuations was significantly lower when participants were performing n-back tasks. Moreover, compared with that in the 2-back and 3-back conditions, the DFA exponent of IAF fluctuations was significantly higher in the 0-back condition, although

the difference between the 2-back and 3-back conditions did not reach a significant level (i.e., $p > 0.05$).

The Scale-Free Dynamics and LRTCs in IAF

Scaling laws are ubiquitous in nature, and they pervade physiological, cognitive, and behavioral activities, signifying that no unique characteristic scale dominates the behavior of these systems (He 2014; Kello et al. 2010). In neuroscience, nearly all related studies have focused on the fluctuations of the instantaneous magnitude of neural signals. Apart from these studies, several other studies found

that phase synchrony between remote cortical regions was also scale-free (Botcharova et al. 2015). As far as we know, the current study is the first study that confirms the presence of scale-freeness in the fluctuations of instantaneous electrical frequency (i.e., IAF). This signifies the fact that, like instantaneous magnitude and phase relationship, the IAF also exhibits fluctuations without characteristic scales. This can be explained by the critical cortex hypothesis, which suggests that criticality is associated with optimized information processing and computation (Shew and Plenz 2013).

A critical property of any brain activities is its test–retest reliability. Much lower test–retest reliability signifies that the feature extracted from cortical activities was unreliable, and then attempts to quantify its changes through experimental manipulations would not be trustworthy as its changes might be due to random neuronal dynamics. Here, although the test–retest reliability of the DFA exponent of IAF was much lower over frontal and central regions, it was fairly high over parietal-occipital regions. This may be caused by the fact that alpha magnitude was largest over occipital regions, which indicates that the occipital alpha wave has much higher signal-to-noise ratio (SNR) and is more robust against random noise. The results of the test–retest reliability analysis suggest that the dynamics of IAF possess LRTCs and scale-free behaviors with properties suitable for functional and clinical studies.

State-Dependent IAF Power-Law Exponent Fluctuations in Human

The results of test–retest reliability analysis showed that the DFA exponent of IAF fluctuations may be a stable neurophysiological “trait” biomarker reflecting anatomical properties of the human brain. In Studies 2 and 3, we investigated whether this feature was highly volatile at shorter time scales, dependent on the individuals’ “state”. Thus, the effect of task manipulations on the DFA exponent of IAF fluctuations was explored. In Study 2, compared with the EC condition, the DFA exponent of IAF fluctuations was attenuated in the EO condition. In Study 3, compared with the EO condition, the DFA exponent of IAF fluctuations was significantly lower when participants were performing n-back tasks. Moreover, compared with that in 2-back and 3-back conditions, the DFA exponent of IAF fluctuations was significantly higher in the 0-back condition. Based on these experimental results, we propose that IAF scaling exponent variability forms the basis of an adaptive mechanism in human brain. Compared with a smaller DFA exponent, a larger DFA exponent indicates that autocorrelation attenuates much more slowly, i.e., the system dynamic in the past has much stronger influence over that in the future (Smit et al. 2011). Thus, a smaller DFA exponent signifies less temporal redundancy and more efficient in online information processing (He 2011). The results revealed here were consistent with

previous studies that revealed that, compared with the task-free state, the power-law exponent of neural signal fluctuations of certain cortical regions and phase synchrony between different cortical regions decreased during task activation (Botcharova et al. 2015; He 2011). These findings fit well with the need for the system to process incoming information in an activated state and the need to maintain memory and plan for future during the baseline state.

Rhythmic neural activity in the occipital alpha band is believed to play a crucial role in the selective processing of visual information (Samaha and Postle 2015; Zumer et al. 2014). Researchers suggested that IAF may reflect the temporal density of periods of maximal perceptual sensitivity and the rate at which visual information is sampled and processed (Samaha and Postle 2015). Thus, the IAF should index the efficiency of information processing on a finer temporal scale than the more sustained transitions associated with alpha magnitude modulations. Compared with the EC condition, the neuronal oscillations should possess less temporal redundancy with more efficient online information processing (i.e., reduced DFA exponent/LRTCs) in the EO condition. Similar to this claim, the DFA exponent of IAF fluctuations should be broken down when participants were performing n-back tasks, compared with that of IAF when they were in EO resting-state. These predictions were confirmed by the results of Study 2 and Study 3.

A confusing result of Study 3 is that, compared with the DFA exponent of IAF fluctuations in the 2-back and 3-back conditions, the DFA exponent of IAF fluctuations was significantly higher in the 0-back condition, whereas the difference between the 2-back and 3-back did not reach a significant level (i.e., $p > 0.05$). This result could be explained by the following account. In the 0-back condition, the participants should respond as quickly as possible when they see the stimulus presented on the screen without identifying what the stimulus is. In the 2-back or 3-back conditions, the participants should identify whether the stimulus currently displayed matches the 2 or 3 preceding stimuli respectively, which need even less temporal redundancy and enhanced efficiency of online visual information processing (i.e., reduced DFA exponent/LRTCs). The difference between the DFA exponent of IAF fluctuations of 2-back and that of 3-back did not reach a significant level may be due to the fact that the visual information processing demands between these two conditions were very similar. This account was further confirmed by the correlation analysis of the DFA exponent of IAF fluctuations and RT. The Pearson’s correlation coefficient between the DFA exponent and the DFA exponent of IAF fluctuations was significant in the 0-back condition, whereas it was not significant in the 2-back condition and 3-back condition. In the 0-back condition, the RT was mainly determined by the efficiency of online visual information processing: the higher visual processing

efficiency (i.e., smaller DFA exponent/LRTCs), the shorter RT. In the 2-back and 3-back conditions, the RTs of participants were determined by quite a few cognitive processes (such as visual processing, working memory update/maintenance/readout) and scale-free properties of IAF fluctuations were not associated with all of these processes.

Limitations and Further Directions

The limitations of this study need to be mentioned. Firstly, Studies 1 and Study 3 included the EEG and behavioral data of only 25/26 participants. Enlarging the sample size should increase the reproducibility of current studies. Secondly, we only studied the monofractal structure of IAF fluctuations. Here, the scale-free feature of IAF fluctuations was defined by a single power law exponent. We assume that the scale invariance is independent of time. However, temporal variation in the scale invariant structure of biomedical signals often appears and could be assessed by a multifractal spectrum of power law exponents using multifractal detrended fluctuation analysis (MFDFA) (Ihlen 2012). In the following studies, we should investigate the multifractal structures of IAF fluctuations, which may reveal some interesting results. Thirdly, in the future, we should test whether the scaling properties of IAF fluctuations could be modulated by other factors, such as age, genetic inheritance, neurological disorders and personality traits.

Conclusion

The scaling properties of the IAF were unraveled through three studies here. Firstly, scale-free behavior was inherent in IAF fluctuations, whether in the EC/EO resting state or the visual working memory task. Secondly, the test–retest reliability of the scaling exponent of IAF fluctuations was fairly high over the parietal-occipital region. This suggests that the scaling exponent of IAF fluctuations may be a stable neurophysiological trait biomarker. Thirdly, the demands for efficiency of online visual information processing could modulate the scaling exponent/LRTCs of IAF fluctuations, which indicates that this feature of IAF is also dependent on the individuals' state.

Acknowledgements The work was supported by Post-funded Project of the National Social Science Fund under Grant 20FJKB005, Henan Province Philosophy and Social Sciences Outstanding Scholars Project under Grant 2018-YXXZ-03, the Philosophy and Social Sciences Planning Project of Henan Province under Grant 2020BJY010, Post-graduate Cultivating Innovation and Quality Improvement Action Plan of Henan University under Grant SYLYC2022039 and Henan University Philosophy and Social Science Innovation Team under Grant 2019CXTD009.

Author Contributions HJ: Conceptualization, methodology, formal analysis, writing—original draft. XW: Formal analysis, writing—original draft. EW: Supervision, funding acquisition, writing—review & editing. HW: Data curation, formal analysis, writing—review & editing. FG: Conceptualization, supervision, data curation, formal analysis, methodology, writing—review & editing.

Data Availability The datasets of Study 1 and Study 2 are available from the corresponding authors upon reasonable request subject to a formal data sharing agreement with Prof. Fei Gao and Prof. Hua Wei. The dataset of Study 3 are available at http://doc.ml.tu-berlin.de/simultaneous_EEG_NIRS/.

Code Availability The MATLAB code here is available from the corresponding author, Prof. Fei Gao, upon reasonable request.

Declarations

Conflict of interest The authors have no relevant financial or non-financial interests to disclose.

Ethical Approval The experimental procedures were approved by the local ethics committee of Peking University People's Hospital (Study 1), Nanjing University (Study 2) and Berlin Institute of Technology (Study 3).

Consent to Participate All participants gave their written informed consent.

References

- Adrian ED, Matthews BHC (1934) The Berger rhythm: potential changes from the occipital lobes in man. *Brain* 57:355–385
- Ahern GL, Schwartz GE (1985) Differential lateralization for positive and negative emotion in the human brain: EEG. *Spectr Anal Neuropsychol* 23:745–755. [https://doi.org/10.1016/0028-3932\(85\)90081-8](https://doi.org/10.1016/0028-3932(85)90081-8)
- Berthouze L, James LM, Farmer SF (2010) Human EEG shows long-range temporal correlations of oscillation amplitude in Theta, Alpha and Beta bands across a wide age range. *Clin Neurophysiol* 121:1187–1197. <https://doi.org/10.1016/j.clinph.2010.02.163>
- Botcharova M, Farmer SF, Berthouze L (2013) A maximum likelihood based technique for validating detrended fluctuation analysis (MFDFA). <https://arXiv.org/1306.5075>
- Botcharova M, Berthouze L, Brookes MJ, Barnes GR, Farmer SF (2015) Resting state MEG oscillations show long-range temporal correlations of phase synchrony that break down during finger movement. *Front Physiol* 6:183. <https://doi.org/10.3389/fphys.2015.00183>
- Cecere R, Rees G, Romei V (2015) Individual differences in alpha frequency drive crossmodal illusory perception. *Curr Biol* 25:231–235. <https://doi.org/10.1016/j.cub.2014.11.034>
- Chen B et al (2015) Individual variability and test-retest reliability revealed by ten repeated resting-state brain scans over one month. *PLoS ONE* 10:e0144963. <https://doi.org/10.1371/journal.pone.0144963>
- Ciuciu P, Abry P, He BJ (2014) Interplay between functional connectivity and scale-free dynamics in intrinsic fMRI networks. *Neuroimage* 95:248–263. <https://doi.org/10.1016/j.neuroimage.2014.03.047>
- Cohen MX (2014) Fluctuations in oscillation frequency control spike timing and coordinate neural networks. *J Neurosci* 34:8988–8998. <https://doi.org/10.1523/JNEUROSCI.0261-14.2014>

- Delorme A, Makeig S (2004) EEGLAB: an open source toolbox for analysis of single-trial EEG dynamics including independent component analysis. *J Neurosci Methods* 134:9–21. <https://doi.org/10.1016/j.jneumeth.2003.10.009>
- Dickinson A, DiStefano C, Senturk D, Jeste SS (2018) Peak alpha frequency is a neural marker of cognitive function across the autism spectrum European. *J Neurosci* 47:643–651. <https://doi.org/10.1111/ejn.13645>
- Gabard-Durnam L, Tierney AL, Vogel-Farley V, Tager-Flusberg H, Nelson CA (2013) Alpha asymmetry in infants at risk for autism spectrum disorders. *J Autism Dev Disord* 45:473–480. <https://doi.org/10.1007/s10803-013-1926-4>
- Haegens S, Cousijn H, Wallis G, Harrison PJ, Nobre AC (2014) Inter- and intra-individual variability in alpha peak frequency. *NeuroImage* 92:46–55. <https://doi.org/10.1016/j.neuroimage.2014.01.049>
- Hahn T et al (2012) Randomness of resting-state brain oscillations encodes Gray's personality trait. *Neuroimage* 59:1842–1845. <https://doi.org/10.1016/j.neuroimage.2011.08.042>
- Hardstone R, Poil SS, Schiavone G, Jansen R, Nikulin VV, Mansvelder HD, Linkenkaer-Hansen K (2012) Detrended fluctuation analysis: a scale-free view on neuronal oscillations. *Front Physiol* 3:450. <https://doi.org/10.3389/fphys.2012.00450>
- He BJ (2011) Scale-free properties of the functional magnetic resonance imaging signal during rest and task. *J Neurosci* 31:13786–13795. <https://doi.org/10.1523/JNEUROSCI.2111-11.2011>
- He BJ (2014) Scale-free brain activity: past, present, and future. *Trends Cogn Sci* 18:480–487. <https://doi.org/10.1016/j.tics.2014.04.003>
- Hu L, Peng W, Valentini E, Zhang ZG, Hu Y (2013) Functional features of nociceptive-induced suppression of alpha band electroencephalographic oscillations. *J Pain* 14:89–99. <https://doi.org/10.1016/j.jpain.2012.10.008>
- Ihlen EAF (2012) Introduction to multifractal detrended fluctuation analysis in Matlab. *Front Physiol* 3:141
- Jann K, Koenig T, Dierks T, Boesch C, Federspiel A (2010) Association of individual resting state EEG alpha frequency and cerebral blood flow. *NeuroImage* 51:365–372. <https://doi.org/10.1016/j.neuroimage.2010.02.024>
- Jia H, Yu D (2019) Attenuated long-range temporal correlations of electrocortical oscillations in patients with autism spectrum disorder. *Dev Cogn Neurosci* 39:100687. <https://doi.org/10.1016/j.dcn.2019.100687>
- Jia H, Peng W, Hu L (2015) A novel approach to identify time-frequency oscillatory features in electrocortical signals. *J Neurosci Methods* 253:18–27. <https://doi.org/10.1016/j.jneumeth.2015.05.026>
- Jia H, Li Y, Yu D (2018) Attenuation of long-range temporal correlations of neuronal oscillations in young children with autism spectrum disorder. *Neuroimage: Clin* 20:424–432. <https://doi.org/10.1016/j.nicl.2018.08.012>
- Kello CT, Brown GDA, Ferrer-i-Cancho R, Holden JG, Linkenkaer-Hansen K, Rhodes T, Van Orden GC (2010) Scaling laws in cognitive sciences. *Trends Cogn Sci* 14:223–232. <https://doi.org/10.1016/j.tics.2010.02.005>
- Klimesch W (1999) EEG alpha and theta oscillations reflect cognitive and memory performance: a review and analysis. *Brain Res Rev* 29:169–195. doi:[https://doi.org/10.1016/S0165-0173\(98\)00056-3](https://doi.org/10.1016/S0165-0173(98)00056-3)
- Lei X, Zhao Z, Chen H (2013) Extraversion is encoded by scale-free dynamics of default mode network. *NeuroImage* 74:52–57. <https://doi.org/10.1016/j.neuroimage.2013.02.020>
- Linkenkaer-Hansen K, Nikouline VV, Palva JM, Ilmoniemi RJ (2001) Long-range temporal correlations and scaling behavior in human brain oscillations. *J Neurosci* 21:1370–1377. <https://doi.org/10.1523/JNEUROSCI.21-04-01370.2001>
- Linkenkaer-Hansen K et al (2007) Genetic contributions to long-range temporal correlations in ongoing oscillations. *J Neurosci* 27:13882–13889. <https://doi.org/10.1523/JNEUROSCI.3083-07.2007>
- Montez T et al (2009) Altered temporal correlations in parietal alpha and prefrontal theta oscillations in early-stage Alzheimer disease. *Proc Natl Acad Sci USA* 106:1614–1619. <https://doi.org/10.1073/pnas.0811699106>
- Nelli S, Itthipuripat S, Srinivasan R, Serences JT (2017) Fluctuations in instantaneous frequency predict alpha amplitude during visual perception. *Nat Commun* 8:2071. <https://doi.org/10.1038/s41467-017-02176-x>
- Nieber D, Schlegel S (1992) Relationships between psychomotor retardation and EEG power spectrum in major depress. *Neuropsychobiology* 25:20–23. <https://doi.org/10.1159/000118804>
- Peng CK, Havlin S, Stanley HE, Goldberger AL (1995) Quantification of scaling exponents and crossover phenomena in nonstationary heartbeat time series. *Chaos* 5:82–87. <https://doi.org/10.1063/1.166141>
- Peng W, Hu L, Zhang Z, Hu Y (2012) Causality in the association between P300 and alpha event-related desynchronization. *PLoS ONE* 7:e34163. <https://doi.org/10.1371/journal.pone.0034163>
- Samaha J, Postle BR (2015) The speed of alpha-band oscillations predicts the temporal resolution of visual perception. *Curr Biol* 25:2985–2990. <https://doi.org/10.1016/j.cub.2015.10.007>
- Samaha J, Bauer P, Cimaroli S, Postle BR (2015) Top-down control of the phase of alpha-band oscillations as a mechanism for temporal prediction. *Proc Natl Acad Sci USA* 112:8439–8444. <https://doi.org/10.1073/pnas.1503686112>
- Sampat MP, Whitman GJ, Stephens TW, Broemeling LD, Heger NA, Bovik AC, Markey MK (2006) The reliability of measuring physical characteristics of spiculated masses on mammography british. *J Radiol* 79:S134–S140. <https://doi.org/10.1259/bjr/96723280>
- Shew WL, Plenz D (2013) The functional benefits of criticality in the cortex. *Neuroscientist* 19:88–100. <https://doi.org/10.1177/1073858412445487>
- Shin J, von Lüthmann A, Kim DW, Mehnert J, Hwang HJ, Müller K-R (2018) Simultaneous acquisition of EEG and NIRS during cognitive tasks for an open access dataset. *Sci Data* 5:180003. <https://doi.org/10.1038/sdata.2018.3>
- Smit DJA et al (2011) Scale-free modulation of resting-state neuronal oscillations reflects prolonged brain maturation in humans. *J Neurosci* 31:13128–13136. <https://doi.org/10.1523/JNEUROSCI.1678-11.2011>
- Zietsch BP, Hansen JL, Hansell NK, Geffen GM, Martin NG, Wright MJ (2007) Common and specific genetic influences on EEG power bands delta, theta, alpha, and beta. *Biol Psychol* 75:154–164. <https://doi.org/10.1016/j.biopsycho.2007.01.004>
- Zumer JM, Scheeringa R, Schoffelen JM, Jensen O (2014) Occipital alpha activity during stimulus processing gates the information flow to object-selective cortex. *PLoS Biol* 12:e1001965. <https://doi.org/10.1371/journal.pbio.1001965>

Publisher's Note Springer Nature remains neutral with regard to jurisdictional claims in published maps and institutional affiliations.

Springer Nature or its licensor (e.g. a society or other partner) holds exclusive rights to this article under a publishing agreement with the author(s) or other rightsholder(s); author self-archiving of the accepted manuscript version of this article is solely governed by the terms of such publishing agreement and applicable law.